

# Global Context Compression with Interleaved Vision-Text Transformation

Dian Jiao<sup>\*†</sup>, Jiaxin Duan<sup>\*</sup>, Shuai Zhao, Jiabing Leng, Yiran Zhang, Feng Huang<sup>‡</sup>

China Electronics Cloud Technology Co., Ltd.

{jiaodian, duanjiaxin, zhaoshuai, lengjiabing, zhangyiran, huangfeng01}@cestc.cn

## Abstract

Recent achievements of vision-language models in end-to-end OCR point to a new avenue for low-loss compression of textual information. This motivates earlier works that render the Transformer’s input into images for prefilling, which effectively reduces the number of tokens through visual encoding, thereby alleviating the quadratically increased Attention computations. However, this partial compression fails to save computational or memory costs at token-by-token inference. In this paper, we investigate global context compression, which saves tokens at both prefilling and inference stages. Consequently, we propose VIST2, a novel Transformer that interleaves input text chunks alongside their visual encoding, while depending exclusively on visual tokens in the pre-context to predict the next text token distribution. Around this idea, we render text chunks into sketch images and train VIST2 in multiple stages, starting from curriculum-scheduled pretraining for optical language modeling, followed by modal-interleaved instruction tuning. We conduct extensive experiments using VIST2 families scaled from 0.6B to 8B to explore the training recipe and hyperparameters. With a  $4\times$  compression ratio, the resulting models demonstrate significant superiority over baselines on long writing tasks, achieving, on average, a  $3\times$  speedup in first-token generation, 77% reduction in memory usage, and 74% reduction in FLOPS. Our codes and datasets will be public to support further studies.

## 1 Introduction

Large language models (LLMs) with Transformer architecture face significant challenges in context scaling because the complexity of self-attention increases quadratically ( $\mathcal{O}(n^2)$ ) with sequence length. This yields an urgent need for *context*

<sup>\*</sup>Equal contributions.

<sup>†</sup>Project leader.

<sup>‡</sup>Corresponding author.

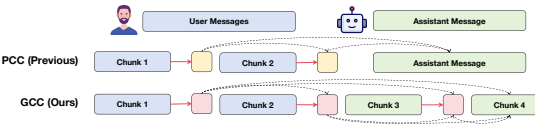


Figure 1: The illustration of context compression of the Transformer. **Right arrow** indicates transforming a text chunk to its latent representation.

*compression* that can reduce computing costs without sacrificing model performance. Existing approaches for context compression are *sparse attention* and *hierarchical encoding*. Following informatics theory, sparse attention (Li et al., 2025a; Beltagy et al., 2020; Lou et al., 2024) drops out detected tokens with marginal information to reduce the Attention operators. In contrast, hierarchical encoding (Cheng et al., 2025; Liu and Qiu, 2025) (in Figure 1) splits a long text into ordered chunks, where each is compressed into densely informative representations. By preserving the complete context, hierarchical encoding effectively prevents information loss, thereby earning widespread interest. Recently, the emerging vision-language models (VLMs), such as dots.ocr (Li et al., 2025c), MinerU-VLM (Wang et al., 2024), and DeepSeek-OCR (Wei et al., 2025) demonstrate remarkable performance in optical character recognition (OCR). The key behind their success - *optical compression* (Li et al., 2025b) opened a new door for a more promising hierarchical encoding. For example, Glyph (Cheng et al., 2025) renders millions of tokens into images and achieved a  $4\times$  lossless compression based on a powerful visual encoder.

Despite these achievements, the mentioned approaches equip LLMs with partial rather than global context compression. Taking the human-AI conversation in Figure 1 as an example, human queries are compressed in prefilling, while the AI responses are generated token-by-token without any compression. In the case of long-text genera-

tion, the model performs intensive computations during training and requires significant memory to store KV-Caches during inference, resulting in considerable costs. To address this problem, we conduct a pioneering exploration for global context compression, aiming to save tokens at both prefilling and inference stages. Specifically, we propose VIST2, a novel Transformer that interleaves text chunks and their optical encoding in input, and predicts the next text token conditioned on visual tokens in pre-context. This interleaved visual-text transformation, named *Optical Language Modeling* (OLM), effectively bridges the gap between partial and global compressions but is often overlooked in existing works. In experiments, VIST2 is implemented using Qwen3 and SigLip2 connected by a linear projection layer. We pretrain this model through several stages, starting with image captioning and OCR to warm up the visual modules, followed by the OLM to adjust the backbone LLM. We then fine-tune it on conversations with long queries and responses, regularized by a modal-interleaved chat template. Extensive results show that our VIST2, with a compression ratio of 4:1, achieves a 3 $\times$  speedup in the first-token delay while also reducing memory usage and FLOPS during inference by over 75% each.

## 2 Background and Problem Definition

This work focuses on text-to-text generation - the general task form of modern linguistic intelligence, which facilitates human-machine interaction through conversations. Given a long input text  $\mathbf{X} = [x_1, x_2, \dots, x_L]$  with the target  $\mathbf{Y} = [y_1, y_2, \dots, y_M]$ , the standard Decoder-only LLMs, e.g., GPT, Llama, Qwen, etc, aim to model the conditional probabilities via next-token prediction:

$$P(\mathbf{Y}|\mathbf{X}) \rightarrow \sum_i^M \mathcal{P}_\theta(y_i|\mathbf{X}, y_{<i}) \quad (1)$$

In the settings where  $L$  and  $M$  exceed the effective context window of standard transformers, the computational complexity increases quadratically, resulting in intensive costs that hinder the training of large language models (LLMs).

**Partial Context Compression** (PCC) methods address this problem by partitioning a long input  $\mathbf{X}$  into  $n$  continuous chunks  $\{\mathcal{C}_i\}_{i=1}^n$ , where each chunk  $\mathcal{C}_i = [x_1^i, \dots, x_k^i]$  contains  $k$  tokens. Additionally, a **text renderer**  $\mathcal{R}(\cdot)$  is employed to

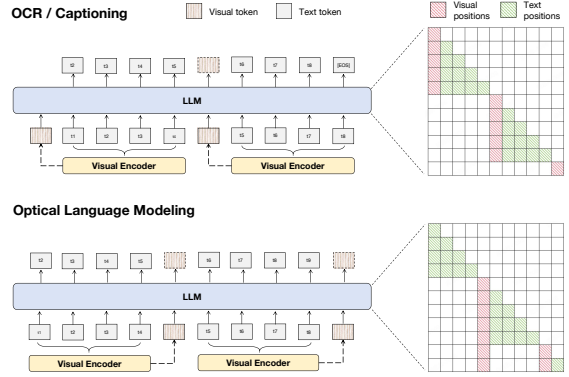


Figure 2: The illustration of pre-training.

render each chunk  $\mathcal{C}_i$  into a grayscale optical image  $\mathcal{V}_i \in \mathbb{R}^{H \times W \times 3}$ . Consequently, they convert the causal language modeling objective in Eq. 1 into visual-language modeling:

$$P(\mathbf{Y}|\mathbf{X}) \rightarrow \sum_i^M \mathcal{P}_\theta(y_i|\{\mathbf{v}_k\}_{k=1}^L, y_{<i}) \quad (2)$$

where  $\mathbf{v}_k = \text{VisualEncoder}(\mathcal{V}_i)$  are visual tokens derived from the chunk  $\mathcal{C}_i$ .

Although PCC extends the context window of Transformers by up to 10 times wider, the visual compression of text tokens works only for prefilling without the support of inference. As a result, PCC enables long-text understanding (LTU), while still facing challenges in long-text generation (LTG), such as storytelling, novel writing, and complicated multi-step reasoning. To address this limitation, we propose *global context compression*, which enables both LTU and LTG through interleaved text-vision compression and vision-text modeling.

## 3 Method: VIST2

**VIST2** is an efficient large language model (LLM) architecture that achieves global context compression by performing iterative visual-text transformations. The core idea behind VIST2 is to utilize the spatial redundancy of rendered text to compress information into a dense visual latent space.

### 3.1 Model Architecture

As illustrated in Figure 1, VIST2 features a sandwich architecture, a popular design in VLMs, comprising a visual encoder (VE) and an LLM backbone connected by a modal aligner.

**Visual Encoder**  $\mathcal{E}(\cdot)$  processes images rendered from structure-free texts into token embeddings. For this reason, we utilize a pretrained Vision

Transformer with the patches sized  $16 \times 16$  (ViT-L/16), which yields  $m = \lfloor \frac{H}{16} \rfloor \times \lfloor \frac{W}{16} \rfloor$  visual tokens per image:

$$\tilde{\mathbf{v}}_i = \mathcal{E}(\hat{\mathcal{V}}_i) \in \mathbb{R}^{m \times d_v}$$

**Modal Aligner**  $\mathcal{M}(\cdot)$  aligns the outputs of VE with the LLM’s embedding space, which is achieved through a multilayer perceptron:

$$\hat{\mathbf{v}}_i = \tanh(\tilde{\mathbf{v}}_i W_m + b_m) \in \mathbb{R}^{m \times d_{lm}}$$

where  $W_m \in \mathbb{R}^{d_v \times d_{lm}}$  and  $b_m \in \mathbb{R}^{d_{lm}}$  are trainable parameters.

**Sparse Attention Mechanism.** The final input to the LLM is an interleaved sequence:

$$\mathbf{H} = [\hat{\mathbf{c}}_1, \hat{\mathbf{v}}_1, \hat{\mathbf{c}}_2, \hat{\mathbf{v}}_2, \dots, \hat{\mathbf{v}}_{n-1}, \hat{\mathbf{c}}_n]$$

where  $\hat{\mathbf{c}}_i$  are token embeddings of  $\hat{\mathcal{C}}_i$ . To achieve GCC, we implement a sparse causal attention that constrains token visibility and saves computations. The **attention mask** is illustrated in Figure 2 (lower), where each token’s visibility follows:

$$\text{Mask}(q, k) = \begin{cases} 1 & \text{if } k \in \{\mathbf{c}_i, \tilde{\mathbf{v}}_{<i}\} \text{ for } q \in \tilde{\mathbf{v}}_i \\ \text{Causal} & \text{otherwise} \end{cases}$$

This ensures that visual tokens act as contextual memory accessible to subsequent chunks, but the context itself can not pass to future textual content. Additionally, the **position** of an embedded token converts to:

$$\text{Pos}(j) = \sum |\tilde{\mathbf{v}}_{<i}| + j$$

where  $|\tilde{\mathbf{v}}_i|$  denotes the number of visual tokens in the  $i$ -th preceding chunk, and  $j$  represents the local offset within the current chunk. In this way, both encoding of visual and text tokens share a continuous and modality-agnostic positional space, which is crucial for saving computations in iterative vision-text transformation.

### 3.2 Model Training

The training of VIST2 encounters two main challenges: first, the LLM and VE are well-trained, while the connector is initialized from scratch, resulting in asynchronous optimization of model parameters. Additionally, the modifications to attention layers pose further challenges over the standard LLM fine-tuning. To address these challenges, we propose a multi-stage training recipe, including staged pre-training and instruction-based fine-tuning. Table 1 reports the details.

#### 3.2.1 Pre-training

We first pretrain VIST2 for image captioning to warm up the modal aligner, with VE and LLM frozen. Subsequently, we train VIST2 with a multi-turn OCR (MT-OCR) task to enable VE for text compression. Specifically, we flip the adjacent odd and even positions in the LLM input:  $\mathbf{H} \rightarrow \tilde{\mathbf{H}} = [\hat{\mathbf{v}}_1, \hat{\mathbf{c}}_1, \hat{\mathbf{v}}_2, \hat{\mathbf{c}}_2, \dots, \hat{\mathbf{v}}_n, \hat{\mathbf{c}}_n]$ . MT-OCR asks the model to recover the content of text chunks conditioned on their optimal features, by minimizing the following training loss:

$$\mathcal{L}_{ocr} = - \sum_{i=1}^n \sum_{j=1}^{|\hat{\mathcal{C}}_i|} \log \mathcal{P}_\theta(u_j^i \mid \{\hat{\mathcal{V}}_k\}_{k < i}, \hat{\mathcal{C}}_{<i}, u_{<j}^i)$$

During this stage, we update the parameters of both VE and the modal aligner with only the LLM frozen. To enhance training convergence, we implement a curriculum schedule for the second stage. It consists of three difficulty levels: easy, which involves OCR of a single image; medium, which encompasses OCR of 2 to 4 images; and hard, which requires OCR of more than 4 images.

After the above two stages, VIST2 is capable of: 1) compressing format-free texts into images with a high compression rate, and 2) recovering the essential texts’ information from their optical images. A further step is required to fit the LLM with sparse attention tailored for the OLM objective in Eq.2. The loss function is:

$$\mathcal{L}_{olm} = - \sum_i^n \sum_{j=1}^{|\hat{\mathcal{C}}_i|} \log \mathcal{P}_\theta(u_j^i \mid \{\hat{\mathcal{V}}_k\}_{k < i}, u_{<j}^i)$$

Figure 2 visualizes the attention masks used in pretraining, conditioned on stages.

#### 3.2.2 Supervised Fine-tuning

We fine-tune VIST2 with *modal-interleaved instruction tuning* to align with real-world applications. This process covers two primary scenarios: (1) long-writing tasks, characterized by concise instructions and extensive narrative responses, and (2) long-context tasks, which involve cumbersome queries but brief outputs (e.g., single-letter answers in "needle-in-a-haystack" benchmarks). Given instruction data in single-turn conversations, we compress the query and response independently, i.e., chunks of size  $K$  are encoded into  $\beta$  visual tokens. To handle the sequence tail, a residual segment of length  $m$  is compressed if  $m > \beta$ ; otherwise, it

remains in its raw tokenized form to preserve fine-grained information. Mathematically, we train the model to minimize the following loss function:

$$\mathcal{L} = - \sum_i^n \sum_{j=1}^{|\hat{\mathcal{C}}_i|} \log \mathcal{P}_\theta(u_j^i \mid \{\hat{\mathcal{V}}_k\}_{k < i}, u_{<j}^i, V(x))$$

In this equation,  $V(x)$  is an input query compressed following the mentioned principle, and the cross-entropy loss is solely sourced from the OLM of the response. Our ablation study reveals that leveraging the pre-trained parameters significantly accelerates convergence on these challenging instruction-following tasks. Please see Appendix 6 for a more comprehensive understanding of the orchestration of our training pipeline.

## 4 Experiment

### 4.1 Experimental Settings

We implement VIST2 using open-source models: with SigLIP2 (Tschanne et al., 2025) as the visual encoder and Qwen3 (Yang et al., 2025) as the backbone LLM. The connector is a randomly initialized multilayer perceptron, with a hidden dimension size of 19,456. In experiments, we keep the visual modules while scaling the size of Qwen3 from 0.6B to 8B, resulting in a family of VIST2 models, named VIST2-0.6B, VIST2-4B, and VIST2-8B. Our experiments are conducted on 8×Nvidia H200 GPUs. Refer to Appendix 1 for the detailed configuration of datasets and hyperparameters.

### 4.2 Pre-training Performance

**Image Captioning.** We pretrain VIST2 on the image captioning task using 690 million open-source samples collected from SA1B\* and CoCo-CN (Li et al., 2019). Since the captioning task converges easily, we terminate the training after the loss stabilizes at  $\sim 0.9$ . Then, we compare the resulting models with powerful VLMs. Table 2 reports the evaluation results on the CoCo test set, with ROUGE scores and CLIPScore (CS) as the matrices. VIST2 performed equivalently with the competitors, indicating the efficient training of the connector.

**Optical Character Recognition.** In the second pre-training stage, we split the WuDao corpora (Yuan et al., 2021) into equal-sized chunks - each consisting of  $L$  continuous tokens - and render them into pure-text images. Specifically,

Table 1: Captioning results after stage-1 pretraining.

Model	Scale	R-1	R-2	R-L	CS
Qwen3-VL	8B	0.309	0.252	0.307	0.4840
InternVL-3.5	8B	0.322	0.251	0.217	0.4863
MiMo-VL	7B	0.327	0.258	0.318	0.4923
Ovis2.5	2.2B	0.221	0.168	0.218	0.3921
Minicpm-4.5V	3B	0.308	0.270	0.302	0.3916
GLM-4.5V	9B	0.335	0.295	0.328	0.4863
VIST2 (ours)	0.6B	0.462	0.318	0.451	0.4901
	4B	0.489	0.342	0.473	0.4881
	8B	0.518	0.369	0.501	0.4867

Table 2: OCR performance after stage-2 pretraining.

Model	Scale	Compression Ratio ( $r$ )				
		2	4	8	10	16
PaddleOCR-VL	0.9B	0.922	0.851	0.817	0.809	0.852
MinerU2.5	1.2B	0.967	0.617	0.619	0.621	0.568
DotsOCR	3B	0.841	0.830	0.846	0.760	0.518
Deepseek-OCR	3B	0.996	0.941	0.986	0.947	0.927
Qwen3-VL	8B	0.521	0.368	0.318	0.370	0.302
Qwen3-VL-SFT	8B	0.988	0.946	0.987	0.930	0.908
VIST2 (ours)	0.6B	0.972	0.983	0.938	0.915	0.890
	4B	0.961	0.942	0.970	0.928	0.905
	8B	0.981	0.950	0.975	0.925	0.912

Table 3: OLM performance after stage-3 pretraining.

Scale	Model	Arxiv	Gutenberg	Wikipedia <sup>†</sup>
0.6B	Qwen3	4.85	4.20	3.95
	VIST2 (ours)	4.98	4.25	4.02
4B	Qwen3	3.22	2.95	2.70
	Qwen3-VL	3.48	3.12	2.82
	VIST2 (ours)	3.25	2.98	2.65
8B	Qwen3	2.15	1.88	1.65
	Qwen3-VL	2.32	2.05	1.78
	VIST2 (ours)	2.22	1.90	1.62

we grid an image into 256 patches to align with the SigLIP2 configuration, which are transformed into 256 optical tokens for the VIST2 input. To find the best compression ratio  $r$ , we set  $L \in [256, 512, 1024, 2048, 2560, 4096]$  (corresponding to  $r \in [1, 2, 4, 8, 10, 16]$ ) and evaluate the OCR performance using ROUGE scores. The training runs on at most  $1024^3$  tokens, and the loss is monitored in Figure 3. It is noticed that a compression ratio less than 10 is not difficult for training convergence. However, when we evaluated the model using 1M tokens excluded from the training partition, the ROUGE-L scores in Table 3 demonstrate that our comparison models suffer from unstable performance with  $r > 4$ . As a result, we set  $r = 4$  in the remaining experiments to facilitate the challenging OLM training.

### 4.3 Fine-tuning Performance

The modal-interleaved instruction tuning is conducted on nearly 10M samples sourced from pub-

\*<https://www.modelscope.cn/datasets/Tongyi-DataEngine/SA1B-Dense-Caption>

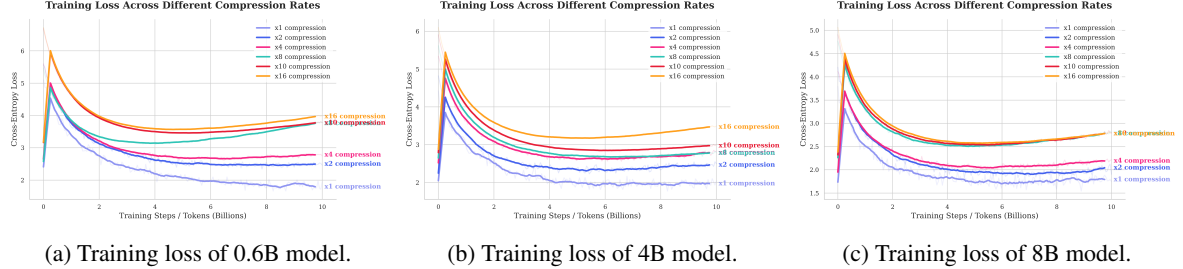


Figure 3: Monitoring stage-2 pre-training loss of VIST2 models.

lically available datasets. The curation of this training set follows three key principles: 1) the samples cover both the Chinese and English languages, 2) each response prepends a chain-of-thought (CoT) within the field surrounded by `<think>` and `</think>` tags before the final answer, and 3) a response is compressed into visual tokens without differentiating CoT and answer. After training, we test the model’s multifaceted performance through extensive evaluations detailed below:

**Long-Context Performance.** We first evaluate the *long-context understanding* of VIST2 using the LongBench benchmark (Bai et al., 2024). As shown in Table 4, VIST2 demonstrates a significant lead over both naive LLMs and existing compression-based methods across all sub-tasks. Specifically, VIST2-8B achieves the highest scores in QA based on single/multiple documents (45.2 and 49.8) and summarization (69.5), outperforming the strong compression baseline AdmTree. Even our smallest variant, VIST2-0.6B, delivers competitive performance in FewShot and Summ tasks, suggesting that our modal-interleaved tuning effectively preserves long-range dependency despite the aggressive visual token compression. Then, we evaluate the *long-text generation* based on the LooGLE benchmark (Li et al., 2024b). The results in Table 5 indicate that VIST2 maintains high generation quality even with a compressed context of 8k×4. In the arXiv paper summarization task, VIST2-8B achieves a GPT4 score of 88.42, which exceeds GPT4-8k (85.42) and GPT3.5-turbo (86.84). For the long dependency QA task, VIST2-8B achieves a RougeL score of 38.12 and a GPT4\_score of 56.45, showcasing its robustness in retrieving and synthesizing information across extremely long sequences. These results validate that compressing responses into visual tokens significantly enhances the ability of the backbone pure-text LLM.

**Fundamental Abilities** are evaluated based on

Table 4: Comparison results on LongBench.

Methods	SglDoc	MtlDoc	Summ.	FewShot	Code
<i>Naive LLM</i>					
Qwen3-4B	25.2	23.8	23.1	65.5	55.9
Qwen3-8B	29.1	24.6	59.4	60.3	42.5
<i>Naive LLM-FT</i>					
Qwen3-4B	36.4	39.3	28.9	68.0	62.7
Qwen3-8B	43.6	38.2	28.3	71.4	63.8
<i>Retrieval-based Methods</i>					
BM25	28.8	31.1	23.8	54.0	32.0
SBERT	18.4	22.9	21.6	50.4	34.6
OpenAI	30.0	19.1	23.8	22.9	51.6
<i>Compression-based Methods</i>					
LongLLMLinguat	24.7	20.3	26.3	55.9	50.1
SnapKV	38.7	37.6	26.2	67.1	60.3
Beacont	40.5	40.3	26.8	68.4	66.4
AdmTree (7B)	41.6	45.9	30.2	<b>69.9</b>	<b>66.8</b>
<i>Ours</i>					
VIST2-0.6B	36.8	39.5	25.2	54.1	58.4
VIST2-4B	<u>41.5</u>	44.2	28.1	<u>60.5</u>	64.9
VIST2-8B	<b>45.2</b>	<b>49.8</b>	<b>30.4</b>	65.2	<u>66.5</u>

four well-known benchmarks: GSM-8k (Cobbe et al., 2021), MATH (Hendrycks et al., 2021), AQUA (Ling et al., 2017), and CMMLU (Li et al., 2024a). We compare VIST2 with naive LLMs and their visual-enhanced counterparts, and the results are reported in Table 6. VIST2 maintains robust general-purpose intelligence across varying scales. On the mathematical reasoning benchmarks GSM-8k and MATH, VIST2-8B achieves scores of 0.87 and 0.30, respectively, slightly underperforming the baseline Qwen3-8B. This suggests that our modal-interleaved pretraining, which takes into account CoT contents in context compression, effectively maintains the model’s thinking capabilities. Furthermore, VIST2-8B scores 0.75 on the Chinese comprehensive benchmark CMMLU, confirming that our bilingual curation principle preserves strong performance in non-English contexts. Overall, these findings indicate that the visual token compression strategy in VIST2 does not sacrifice fundamental LLM capacities, making it a versatile backbone for both long-document parsing and general reasoning tasks.

Table 5: Comparison results on LooGLE.

Models	Context	Bleu1	Bleu4	Rouge1	Rouge4	RougeL	Meteor	Bert_score	GPT4_score
<b>ArXiv Paper Summarization</b>									
GPT4-32k	32k	24.50	0.73	27.15	7.10	24.25	19.03	84.04	82.84
GPT4-8k	8k	29.02	2.09	32.08	11.11	28.85	22.64	84.92	85.42
GPT3.5-turbo-16k	16k	28.70	1.59	32.04	10.69	28.89	22.34	84.82	86.84
Llmalndex	-	22.53	0.63	26.28	6.97	23.73	21.07	83.09	76.35
ChatGLM2-6B	32k	0.04	0.00	5.97	0.00	5.82	6.40	73.25	13.23
LongLLaMa-3B-Instruct	256k	0.00	0.00	0.07	0.00	0.07	0.33	26.01	5.57
RWKV-4-14B-raven	8k	15.51	0.09	18.98	3.32	17.12	14.78	80.05	34.79
LLaMA2-7B-32K-Instruct	32k	0.09	0.00	0.20	0.00	0.20	2.44	72.41	6.14
VIST2-0.6B	8k $\times$ 4	26.12	1.10	29.45	8.54	26.15	20.12	83.95	81.20
VIST2-4B	8k $\times$ 4	28.45	1.88	31.80	10.42	28.52	22.10	84.70	86.15
VIST2-8B	8k $\times$ 4	29.15	2.15	33.24	11.45	29.75	22.88	85.12	88.42
<b>Long Dependency QA</b>									
GPT4-32k	32k	8.55	1.40	25.59	6.36	24.04	11.13	80.16	54.09
GPT4-8k	8k	8.94	1.01	23.45	6.57	21.69	10.18	85.36	42.12
GPT3.5-turbo-16k	16k	6.92	1.81	25.02	6.68	23.63	10.40	83.79	45.04
Llmalndex	-	7.76	1.24	23.62	7.10	22.30	10.47	83.87	37.63
ChatGLM2-6B	32k	5.55	0.11	9.41	1.93	8.69	4.39	85.78	11.50
LongLLaMa-3B-Instruct	256k	5.64	0.49	17.30	3.76	16.29	6.53	84.26	21.64
RWKV-4-14B-raven	8k	3.88	0.22	20.39	3.20	19.20	6.41	81.46	14.32
LLaMA2-7B-32K-Instruct	32k	0.08	0.00	4.07	0.00	4.07	1.06	66.54	2.85
Claude3-opus	200k	3.28	0.43	37.95	13.46	36.56	9.44	79.58	20.71
VIST2-0.6B	8k $\times$ 4	8.12	0.95	35.10	11.20	33.45	9.85	82.15	48.30
VIST2-4B	8k $\times$ 4	9.05	1.55	38.65	13.50	37.10	10.82	84.60	54.12
VIST2-8B	8k $\times$ 4	9.42	1.78	40.12	14.22	38.12	11.45	85.34	56.45

Table 6: Evaluation results of general performance.

Methods	GSM-8k	MATH	AQUA	CMMLU
<i>Naive LLM</i>				
Qwen3-4B	0.8597	0.2559	0.2840	0.7025
Qwen3-8B	0.8842	0.3120	0.3345	0.7680
<i>Visual-enhanced LLM</i>				
Qwen3-VL-4B	0.7180	0.8583	0.2596	0.6542
Qwen3-VL-8B	0.7855	0.8924	0.2988	0.7135
<i>Ours</i>				
VIST2-4B	0.8431	0.2485	0.2795	0.6950
VIST2-8B	0.8715	0.3015	0.3210	0.7512

**Optical Language Modeling.** OLM requires our VIST2 to continue the content of spaced chunks conditioned solely on their optical representations. To achieve this, we gather long documents (exceeding 8k tokens) from three corpora: Arxiv (Li et al., 2024c), Gutenberg<sup>†</sup>, and WuDao (Yuan et al., 2021), to create a training set. After training, we evaluate the resulting model by providing the first 1k tokens of a document and using the perplexity calculated by GPT-4 to quantify model performance in writing the remaining content (at most 4k output tokens). Results in Table 3 indicate that: 1) The existing foundational vision-language model is inadequate for the continuation of long texts. 2) After the training with OLM, the long-writing performance of VIST2 surpasses the VLM encounters by 0.2~0.5 on average, which is close to the baseline pure language models.

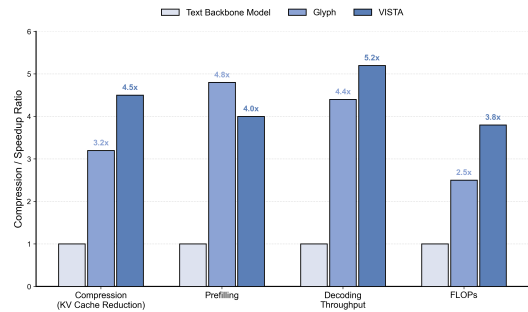


Figure 4: Comparison of efficiency.

#### 4.4 Efficiency Analysis

In Figure 4, we compare VIST2 with another optical context compression approach, Glyph, in terms of savings in computing and memory cost, as well as improvements in responding speed and throughput. Note that VIST2 and Glyph share a similar compression ratio ( $\sim 4 \times$ ), and the two models represent PCC and GCC, respectively. GCC presents a significant advantage in KV-Cache saving and FLOPs reduction. The two models have an equivalent throughput, and VIST2 achieves a slightly lower prefiling compression because it is implemented with a fixed compression ratio, without an enhanced visual encoder or an adaptive compression mechanism, which is left for future work.

## 5 Conclusion

In this work, we conduct a pioneering investigation of global context compression (GCC). Additionally,

<sup>†</sup><https://www.gutenberg.org/>

we propose VIST2, a novel Transformer architecture that achieves GCC with interleaved vision-text transformation. The key technique of VIST2 is a staged training recipe that connects the advanced modal-interleaved instruction tuning and the basic visual-language tasks with optical language modeling. As a result, VIST2 presents higher efficiency in saving computing and memory costs than previous PCC approaches, while maintaining advances in long text understanding and generation.

## 6 Future Works

While VIST2 demonstrates a substantial leap in efficient optical-based context compression, several promising avenues for future research remain:

- **Specialized Visual Encoders for Texts.** In this work, VIST2 utilizes a general-purpose visual encoder that has not been specifically optimized for the high-density textual information found in documents. Future iterations could explore the integration of document-centric visual models (e.g., specialized CLIP-style variants trained on academic or structured text) to achieve even higher semantic compression ratios without compromising granular details.
- **Content-Aware Adaptive Compression.** Our current framework employs a static compression law based on fixed-size chunking. However, document regions vary significantly in information density (e.g., blank margins vs. complex tables). Implementing an adaptive compression mechanism - one that dynamically allocates visual tokens based on the local informativeness or structural complexity of each chunk - could further optimize the trade-off between computational efficiency and reconstruction fidelity.
- **Modal-interleaved Reinforcement Learning.** This study focuses on the pre-training and supervised fine-tuning of VIST2. A natural next step is to investigate alignment techniques based on reinforcement learning, specifically tailored for modal-interleaved contexts. Such alignment could better harmonize the reasoning process with the verifiable rewards.

## References

Shuai Bai, Yuxuan Cai, Ruizhe Chen, Keqin Chen, Xionghui Chen, Zesen Cheng, Lianghao Deng, Wei

Ding, Chang Gao, Chunjiang Ge, Wenbin Ge, Zhi-fang Guo, Qidong Huang, Jie Huang, Fei Huang, Binyuan Hui, Shutong Jiang, Zhaohai Li, Ming-sheng Li, Mei Li, Kaixin Li, Zicheng Lin, Junyang Lin, Xuejing Liu, Jiawei Liu, Chenglong Liu, Yang Liu, Dayiheng Liu, Shixuan Liu, Dunjie Lu, Ruilin Luo, Chenxu Lv, Rui Men, Lingchen Meng, Xu-ancheng Ren, Xingzhang Ren, Sibo Song, Yuchong Sun, Jun Tang, Jianhong Tu, Jianqiang Wan, Peng Wang, Pengfei Wang, Qiuyue Wang, Yuxuan Wang, Tianbao Xie, Yiheng Xu, Haiyang Xu, Jin Xu, Zhibo Yang, Mingkun Yang, Jianxin Yang, An Yang, Bowen Yu, Fei Zhang, Hang Zhang, Xi Zhang, Bo Zheng, Humen Zhong, Jingren Zhou, Fan Zhou, Jing Zhou, Yuanzhi Zhu, and Ke Zhu. 2025. *Qwen3-vl technical report*. Preprint, arXiv:2511.21631.

Yushi Bai, Xin Lv, Jiajie Zhang, Hongchang Lyu, Jiankai Tang, Zhidian Huang, Zhengxiao Du, Xiao Liu, Aohan Zeng, Lei Hou, Yuxiao Dong, Jie Tang, and Juanzi Li. 2024. *Longbench: A bilingual, multi-task benchmark for long context understanding*. In *Proceedings of the 62nd Annual Meeting of the Association for Computational Linguistics (Volume 1: Long Papers), ACL 2024, Bangkok, Thailand, August 11-16, 2024*, pages 3119–3137. Association for Computational Linguistics.

Iz Beltagy, Matthew E. Peters, and Arman Cohan. 2020. *Longformer: The long-document transformer*. Preprint, arXiv:2004.05150.

Jiale Cheng, Yusen Liu, Xinyu Zhang, Yulin Fei, Wenyi Hong, Ruiliang Lyu, Weihan Wang, Zhe Su, Xiaotao Gu, Xiao Liu, Yushi Bai, Jie Tang, Hongning Wang, and Minlie Huang. 2025. *Glyph: Scaling context windows via visual-text compression*. CoRR, abs/2510.17800.

Karl Cobbe, Vineet Kosaraju, Mohammad Bavarian, Mark Chen, Heewoo Jun, Lukasz Kaiser, Matthias Plappert, Jerry Tworek, Jacob Hilton, Reichiro Nakano, Christopher Hesse, and John Schulman. 2021. Training verifiers to solve math word problems. *arXiv preprint arXiv:2110.14168*.

Cheng Cui, Ting Sun, Suyin Liang, Tingquan Gao, Zelun Zhang, Jiaxuan Liu, Xueqing Wang, Changda Zhou, Hongen Liu, Manhui Lin, Yue Zhang, Yubo Zhang, Handong Zheng, Jing Zhang, Jun Zhang, Yi Liu, Dianhai Yu, and Yanjun Ma. 2025. *Paddleocr-vl: Boosting multilingual document parsing via a 0.9b ultra-compact vision-language model*. Preprint, arXiv:2510.14528.

Dan Hendrycks, Collin Burns, Saurav Kadavath, Akul Arora, Steven Basart, Eric Tang, Dawn Song, and Jacob Steinhardt. 2021. Measuring mathematical problem solving with the math dataset. *arXiv preprint arXiv:2103.03874*.

Haonan Li, Yixuan Zhang, Fajri Koto, Yifei Yang, Hai Zhao, Yeyun Gong, Nan Duan, and Timothy Baldwin. 2024a. *CMLU: measuring massive multitask language understanding in chinese*. In *Findings of*

*the Association for Computational Linguistics, ACL 2024, Bangkok, Thailand and virtual meeting, August 11-16, 2024, pages 11260–11285. Association for Computational Linguistics.*

Jiaqi Li, Mengmeng Wang, Zilong Zheng, and Muhan Zhang. 2024b. **Google: Can long-context language models understand long contexts?** In *Proceedings of the 62nd Annual Meeting of the Association for Computational Linguistics (Volume 1: Long Papers), ACL 2024, Bangkok, Thailand, August 11-16, 2024, pages 16304–16333. Association for Computational Linguistics.*

Lei Li, Yuqi Wang, Runxin Xu, Peiyi Wang, Xiaochong Feng, Lingpeng Kong, and Qi Liu. 2024c. **Multimodal arxiv: A dataset for improving scientific comprehension of large vision-language models.** *Preprint*, arXiv:2403.00231.

Xirong Li, Chaoxi Xu, Xiaoxu Wang, Weiyu Lan, Zhengxiong Jia, Gang Yang, and Jieping Xu. 2019. **Coco-cn for cross-lingual image tagging, captioning and retrieval.** *Preprint*, arXiv:1805.08661.

Yangning Li, Shaoshen Chen, Yinghui Li, Yankai Chen, Hai-Tao Zheng, Hui Wang, Wenhao Jiang, and Philip S Yu. 2025a. **Admtree: Compressing lengthy context with adaptive semantic trees.** *arXiv preprint arXiv:2512.04550*.

Yanhong Li, Zixuan Lan, and Jiawei Zhou. 2025b. **Text or pixels? it takes half: On the token efficiency of visual text inputs in multimodal llms.** *CoRR*, abs/2510.18279.

Yumeng Li, Guang Yang, Hao Liu, Bowen Wang, and Colin Zhang. 2025c. **dots.ocr: Multilingual document layout parsing in a single vision-language model.** *Preprint*, arXiv:2512.02498.

Wang Ling, Dani Yogatama, Chris Dyer, and Phil Blunsom. 2017. **Program induction by rationale generation: Learning to solve and explain algebraic word problems.** In *Proceedings of the 55th Annual Meeting of the Association for Computational Linguistics, ACL 2017, Vancouver, Canada, July 30 - August 4, Volume 1: Long Papers*, pages 158–167. Association for Computational Linguistics.

Fanfan Liu and Haibo Qiu. 2025. **Context cascade compression: Exploring the upper limits of text compression.** *arXiv preprint arXiv:2511.15244*.

Chao Lou, Zixia Jia, Zilong Zheng, and Kewei Tu. 2024. **Sparser is faster and less is more: Efficient sparse attention for long-range transformers.** *CoRR*, abs/2406.16747.

Shiyin Lu, Yang Li, Yu Xia, Yuwei Hu, Shanshan Zhao, Yanqing Ma, Zhichao Wei, Yinglun Li, Lunhao Duan, Jianshan Zhao, Yuxuan Han, Haijun Li, Wanying Chen, Junke Tang, Chengkun Hou, Zhixing Du, Tianli Zhou, Wenjie Zhang, Huping Ding, Jiahe Li, Wen Li, Gui Hu, Yiliang Gu, Siran Yang, Jiamang Wang, Hailong Sun, Yibo Wang,

Hui Sun, Jinlong Huang, Yuping He, Shengze Shi, Weihong Zhang, Guodong Zheng, Junpeng Jiang, Sensen Gao, Yi-Feng Wu, Sijia Chen, Yuhui Chen, Qing-Guo Chen, Zhao Xu, Weihua Luo, and Kaifu Zhang. 2025. **Ovis2.5 technical report.** *Preprint*, arXiv:2508.11737.

Arsenii Moskvichev and Ky-Vinh Mai. 2023. **NarrativeXL: a large-scale dataset for long-term memory models.** In *Findings of the Association for Computational Linguistics: EMNLP 2023*, pages 15058–15072, Singapore. Association for Computational Linguistics.

Core Team, Zihao Yue, Zhenru Lin, Yifan Song, Weikun Wang, Shuhuai Ren, Shuhao Gu, Shicheng Li, Peidian Li, Liang Zhao, Lei Li, Kainan Bao, Hao Tian, Hailin Zhang, Gang Wang, Dawei Zhu, Cici, Chenhong He, Bowen Ye, Bowen Shen, Zihan Zhang, Zihan Jiang, Zhixian Zheng, Zhichao Song, Zhenbo Luo, Yue Yu, Yudong Wang, Yuanyuan Tian, Yu Tu, Yihan Yan, Yi Huang, Xu Wang, Xinzhe Xu, Xingchen Song, Xing Zhang, Xing Yong, Xin Zhang, Xiangwei Deng, Wenyu Yang, Wenhan Ma, Weiwei Lv, Weiji Zhuang, Wei Liu, Sirui Deng, Shuo Liu, Shimao Chen, Shihua Yu, Shaohui Liu, Shande Wang, Rui Ma, Qiantong Wang, Peng Wang, Nuo Chen, Menghang Zhu, Kangyang Zhou, Kang Zhou, Kai Fang, Jun Shi, Jinhao Dong, Jiebao Xiao, Jiaming Xu, Huaqiu Liu, Hongshen Xu, Heng Qu, Haochen Zhao, Hanglong Lv, Guoan Wang, Duo Zhang, Dong Zhang, Di Zhang, Chong Ma, Chang Liu, Can Cai, and Bingquan Xia. 2025. **Mimo-vl technical report.** *Preprint*, arXiv:2506.03569.

V Team, Wenyi Hong, Wenmeng Yu, Xiaotao Gu, Guo Wang, Guobing Gan, Haomiao Tang, Jiale Cheng, Ji Qi, Junhui Ji, Lihang Pan, Shuaiqi Duan, Weihan Wang, Yan Wang, Yean Cheng, Zehai He, Zhe Su, Zhen Yang, Ziyang Pan, Aohan Zeng, Baoxu Wang, Bin Chen, Boyan Shi, Changyu Pang, Chenhui Zhang, Da Yin, Fan Yang, Guoqing Chen, Haochen Li, Jiale Zhu, Jiali Chen, Jiaxing Xu, Jiazheng Xu, Jing Chen, Jinghao Lin, Jinhao Chen, Jinjiang Wang, Junjie Chen, Leqi Lei, Letian Gong, Leyi Pan, Mingdao Liu, Mingde Xu, Mingzhi Zhang, Qinkai Zheng, Ruiliang Lyu, Shangqin Tu, Sheng Yang, Shengbiao Meng, Shi Zhong, Shiyu Huang, Shuyuan Zhao, Siyan Xue, Tianshu Zhang, Tianwei Luo, Tianxiang Hao, Tianyu Tong, Wei Jia, Wenkai Li, Xiao Liu, Xiaohan Zhang, Xin Lyu, Xinyu Zhang, Xinyue Fan, Xuancheng Huang, Yadong Xue, Yanfeng Wang, Yanling Wang, Yanzi Wang, Yifan An, Yifan Du, Yiheng Huang, Yilin Niu, Yiming Shi, Yu Wang, Yuan Wang, Yuanchang Yue, Yuchen Li, Yusen Liu, Yutao Zhang, Yuting Wang, Yuxuan Zhang, Zhao Xue, Zhengxiao Du, Zhenyu Hou, Zihan Wang, Peng Zhang, Debing Liu, Bin Xu, Juanzi Li, Minlie Huang, Yuxiao Dong, and Jie Tang. 2026. **Glm-4.5v and glm-4.1v-thinking: Towards versatile multimodal reasoning with scalable reinforcement learning.** *Preprint*, arXiv:2507.01006.

Michael Tschanen, Alexey Gritsenko, Xiao Wang, Muhammad Ferjad Naeem, Ibrahim Alabdulmohsin,

Nikhil Parthasarathy, Talfan Evans, Lucas Beyer, Ye Xia, Basil Mustafa, Olivier Hénaff, Jeremiah Harmsen, Andreas Steiner, and Xiaohua Zhai. 2025. **Siglip 2: Multilingual vision-language encoders with improved semantic understanding, localization, and dense features.** *Preprint*, arXiv:2502.14786.

Bin Wang, Chao Xu, Xiaomeng Zhao, Linke Ouyang, Fan Wu, Zhiyuan Zhao, Rui Xu, Kaiwen Liu, Yuan Qu, Fukai Shang, Bo Zhang, Liqun Wei, Zhihao Sui, Wei Li, Botian Shi, Yu Qiao, Dahua Lin, and Conghui He. 2024. **Mineru: An open-source solution for precise document content extraction.** *Preprint*, arXiv:2409.18839.

Weiyun Wang, Zhangwei Gao, Lixin Gu, Hengjun Pu, Long Cui, Xinguang Wei, Zhaoyang Liu, Linglin Jing, Shenglong Ye, Jie Shao, Zhaokai Wang, Zhe Chen, Hongjie Zhang, Ganlin Yang, Haomin Wang, Qi Wei, Jinhui Yin, Wenhao Li, Erfei Cui, Guanzhou Chen, Zichen Ding, Changyao Tian, Zhenyu Wu, Jingjing Xie, Zehao Li, Bowen Yang, Yuchen Duan, Xuehui Wang, Zhi Hou, Haoran Hao, Tianyi Zhang, Songze Li, Xiangyu Zhao, Haodong Duan, Nianchen Deng, Bin Fu, Yinan He, Yi Wang, Conghui He, Botian Shi, Junjun He, Yingtong Xiong, Han Lv, Lijun Wu, Wenqi Shao, Kaipeng Zhang, Huipeng Deng, Biqing Qi, Jiaye Ge, Qipeng Guo, Wenwei Zhang, Songyang Zhang, Maosong Cao, Junyao Lin, Kexian Tang, Jianfei Gao, Haian Huang, Yuzhe Gu, Chengqi Lyu, Huanze Tang, Rui Wang, Haijun Lv, Wanli Ouyang, Limin Wang, Min Dou, Xizhou Zhu, Tong Lu, Dahua Lin, Jifeng Dai, Weijie Su, Bowen Zhou, Kai Chen, Yu Qiao, Wenhui Wang, and Gen Luo. 2025. **Internvl3.5: Advancing open-source multi-modal models in versatility, reasoning, and efficiency.** *Preprint*, arXiv:2508.18265.

Haoran Wei, Yaofeng Sun, and Yukun Li. 2025. **Deepseek-ocr: Contexts optical compression.** *Preprint*, arXiv:2510.18234.

An Yang, Anfeng Li, Baosong Yang, Beichen Zhang, Binyuan Hui, Bo Zheng, Bowen Yu, Chang Gao, Chengan Huang, Chenxu Lv, Chujie Zheng, Dayiheng Liu, Fan Zhou, Fei Huang, Feng Hu, Hao Ge, Haoran Wei, Huan Lin, Jialong Tang, Jian Yang, Jianhong Tu, Jianwei Zhang, Jianxin Yang, Jiaxi Yang, Jing Zhou, Jingren Zhou, Junyang Lin, Kai Dang, Keqin Bao, Kexin Yang, Le Yu, Lianghao Deng, Mei Li, Mingfeng Xue, Mingze Li, Pei Zhang, Peng Wang, Qin Zhu, Rui Men, Ruize Gao, Shixuan Liu, Shuang Luo, Tianhao Li, Tianyi Tang, Wenbiao Yin, Xingzhang Ren, Xinyu Wang, Xinyu Zhang, Xuanancheng Ren, Yang Fan, Yang Su, Yichang Zhang, Yinger Zhang, Yu Wan, Yuqiong Liu, Zekun Wang, Zeyu Cui, Zhenru Zhang, Zhipeng Zhou, and Zihan Qiu. 2025. **Qwen3 technical report.** *Preprint*, arXiv:2505.09388.

Tianyu Yu, Zefan Wang, Chongyi Wang, Fuwei Huang, Wenshuo Ma, Zhihui He, Tianchi Cai, Weize Chen, Yuxiang Huang, Yuanqian Zhao, Bokai Xu, Junbo Cui, Yingjing Xu, Liqing Ruan, Luoyuan Zhang, Hanyu Liu, Jingkun Tang, Hongyuan Liu, Qining Guo, Wenhao Hu, Bingxiang He, Jie Zhou, Jie Cai, Ji Qi, Zonghao Guo, Chi Chen, Guoyang Zeng, Yuxuan Li, Ganqu Cui, Ning Ding, Xu Han, Yuan Yao, Zhiyuan Liu, and Maosong Sun. 2025. **Minicpm-v 4.5: Cooking efficient mllms via architecture, data, and training recipe.** *Preprint*, arXiv:2509.18154.

Sha Yuan, Hanyu Zhao, Zhengxiao Du, Ming Ding, Xiao Liu, Yukuo Cen, Xu Zou, Zhilin Yang, and Jie Tang. 2021. **Wudaocorpora: A super large-scale chinese corpora for pre-training language models.** *AI Open*, 2:65–68.

## A Experimental Settings

### A.1 Image Captioning

To evaluate the model performance of image captioning, we compare VIST2 with six naive VLMs:

**Qwen3-VL** (Bai et al., 2025): Qwen3-VL family utilizes an enhanced interleaved-MROPE for spatial-temporal modeling and supports native interleaved contexts of up to 256K tokens for long-context comprehension of documents and videos.

**InternVL-3.5** (Wang et al., 2025): Featuring a Cascade Reinforcement Learning framework and a Visual Resolution Router, this open-source series achieves state-of-the-art results by balancing advanced reasoning capabilities with high inference efficiency.

**MiMo-VL** (Team et al., 2025): MiMo-VL is a multimodal model designed to bridge the gap between open-source and commercial models through advanced reinforcement learning techniques focused on general multimodal and agentic tasks.

**Ovis2.5** (Lu et al., 2025): Ovis2.5 is a high-performance vision-language model that employs a structural alignment strategy to better process high-resolution images and complex visual reasoning tasks.

**Minicpm-4.5V** (Yu et al., 2025): MiniCPM-V 4.5 is a versatile, end-side multimodal model that provides strong OCR and multimodal understanding capabilities while maintaining a compact parameter size for efficient deployment.

**GLM-4.5V** (Team et al., 2026): GLM-4.5V is a large-scale multimodal model that excels in multidisciplinary reasoning and high-resolution document understanding, rivaling leading commercial models in its perception and generation quality.

### A.2 Optical Character Recognition

To evaluate the model performance of optical character recognition, we compare VIST2 with four VLMs tailored for OCR, apart from the naive Qwen3-VL and the Qwen3-VL fine-tuned on our dataset:

**PaddleOCR-VL** (Cui et al., 2025): This ultra-compact 0.9B parameter model integrates a NaViT-style dynamic resolution visual encoder with the ERNIE-4.5-0.3B language model to achieve state-of-the-art efficiency in multilingual document parsing across 109 languages.

**MinerU2.5** (Wang et al., 2024): MinerU2.5 employs a decoupled two-stage framework that separates global layout analysis from local content

recognition, enabling high-resolution parsing of complex elements like formulas and tables with minimal computational overhead.

**DotsOCR** (Li et al., 2025c): This unified 1.7B-parameter vision-language model is designed to jointly learn layout detection, content recognition, and relational understanding within a single end-to-end pass, providing robust performance on the XDocParse benchmark.

**Deepseek-OCR** (Wei et al., 2025): Deepseek-OCR introduces the concept of "context optical compression," utilizing a multi-stage DeepEncoder and a Mixture-of-Experts decoder to compress 2D document pages into a compact set of vision tokens for efficient high-accuracy transcription.

### A.3 Fine-tuning Performance

For the assessment of long-context understanding and long-text generation, we compared VIST2 against models that have publicly available evaluation results. Results in Table 4 are reported in (Li et al., 2025a), and results in Table 5 are reported in (Li et al., 2024b), respectively.

## B Implementation Details

**Datasets.** Table 7 presents the datasets utilized in the VIST2 training process, categorized by stages.

At the fine-tuning stage, note that Deepseek-R1-Distill<sup>‡</sup> is already an instruction-following dataset; we filter samples with responses longer than 4,096 tokens to inflate our training set. Additionally, we employ NarrativeXL (Moskvichev and Mai, 2023), a long document comprehension dataset with the letter of the ground-truth option as the target label. We augment it by asking Qwen3<sup>§</sup> to answer the questions after thinking. Only the samples with a format of thought-analysis-option and longer than 2,048 tokens are incorporated into our training data. For the Arxiv, Gutenberg, and WuDao corpora, we extract documents longer than 512 tokens and prompt Qwen3 to generate questions varying in difficulty levels (1 to 5). Subsequently, we instruct Qwen3 to provide answers using a chain-of-thought approach for each document-question pair. Response texts exceeding 2,048 tokens are incorporated into our dataset. During training, we randomly sample 10 million entries from this re-

<sup>‡</sup><https://huggingface.co/datasets/a-m-team/AM-DeepSeek-R1-0528-Distilled>

<sup>§</sup><https://huggingface.co/Qwen/Qwen3-235B-A22B-Thinking-2507>

Table 7: Details of the multi-stage training of VIST2.  $\dagger$ : datasets for long-text understanding.  $\ddagger$ : datasets for long-text generation.

Task	Dataset	Frozen			#Data Volume
		VE	MC	LLM	
<i>Pre-training</i>					
Caption	CoCo, SA1B	✓	✗	✓	690M Images
MT-OCR	WuDao	✗	✗	✓	1B Tokens
OLM	Arxiv, Gutenberg, WuDao	✓	✓	✗	1B Tokens
<i>Fine-tuning</i>					
Instruct-Follow	Arxiv $\dagger$ , Gutenberg $\dagger$ , NarrativeXL $\dagger$ , WuDao $\dagger$ , Deepseek-R1-Distill $\ddagger$	✓	✓	✗	10M Instructions

Table 8: Hyperparameter settings. PT: pre-training. SFT: supervised instruction-tuning.  $\dagger$ : batch size achieved through gradient accumulation.

Stage	PT-1	PT-2	PT-3	SFT
Optimizer				AdamW
Weight Decay				1e-4
Warmup Ratio				0.01
Learning Rate Schedule				Cosine
# of Epochs				1
Learning Rate	5e-4	5e-4	5e-4	1e-5
Batch Size (VIST2-0.6B)	96	64	64 $\dagger$	64 $\dagger$
Batch Size (VIST2-4B)	64	32	16 $\dagger$	16 $\dagger$
Batch Size (VIST2-8B)	48	24	8 $\dagger$	8 $\dagger$
# of Maximum Length	1,024	4,096	8,192	8,192

sulting dataset for modal-interleaved instruction tuning.

**Training Configurations.** Our codes are implemented with Pytorch 2.6.0 and the Huggingface Transformers repository. Table 8 further reports the training configurations.

## C Application Examples

Figure 6 illustrates the usage of VIST2, where the short query remains uncompressed while the lengthy response is effectively compressed into the visual context during the generation process. In addition, Figure 7 demonstrates that the long query is also compressed during context pre-filling. The original 3,784 tokens are reduced to 1,024 visual tokens, resulting in significant savings in the KV-Cache.

## D Ablation of OLM Training

In Figure 5, we examine the necessity of stage-3 pre-training with OLM by monitoring the fine-tuning loss of the VIST2-4B variants. The results indicate that intermediate modal-interleaved instruction tuning using OLM significantly improves training stability, resulting in a smoother convergence of loss.



Figure 5: Training loss of image captioning.

## Unfinished Response

## Continue Response



能给我讲一个寓意深刻的故事吗？



<think>

好的，让我讲一个寓意深刻的故事。首先，我需要确定用户的需求是什么。他们可能想要一个能引发思考、有深层含义的故事，而不仅仅是娱乐性的。接下来，我得考虑故事的题材、寓言、现代故事还是神话改编？用户没有指定，所以可能需要一个通用且容易理解的类型。

然后，主题方面，用户要求寓意深刻，所以需要选择一个普遍的主题，比如生命的意义、自我认知、成长等。考虑到现代人可能面临的困惑，比如存在的意义、工作的重复性，这样的主题更容易引起共鸣。

接下来是角色设定。主角需要 *relatable*，可能是一个普通人、或者象征性的角色，比如机器人。这样更容易带入寓意。机器人有程序设定，却寻求自由。这样的冲突明显，容易展开。

故事结构方面，可能需要一个循环的结构，来强调主题，比如开始和结束在同一个地方，但主角有了新的认识，这样能突出转变和领悟。

然后考虑情节发展。主角觉醒，逃离，经历外面的世界，发现真相，最终回归。这样的结构可以展示变化的过程，并带出寓意，中间的导师角色可以帮助传递主题，比如老园丁的话，暗示生命的意义在于过程而非目的。

在细节描写上，需要加入象征元素，比如编号、机械的工作、自然界的对比，老园丁的沙漏、胡须里的嫩芽。这些意象能增强故事的深度和隐喻。

最后，结尾部分要让主角领悟到真谛，即使回到原地，但心态不同，带出主题：存在的意义在于体验本身，这样用户能得到启示，符合寓意深刻的要求。

需要检查故事是否流畅，有没有逻辑漏洞，以及寓意是否明确。可能还需要调整语言，使其更生动，有画面感，让读者更容易沉浸其中。确保故事不长不短，结构紧凑，结尾点题，让用户回味。

</think>

好的，我将按照您的要求创作一个富有寓意的故事。为了让故事更完整，我会先列出一些基本的情节脉络，请您看看以下内容是否符合您的预期。如果您有其他想法，可以随时提出，我会进行调整。

### ## 世界观设定

- \*“时空背景\*：近未来时空管理局内部，具有永恒循环属性的微观宇宙观测站。

- \*\*“核心矛盾\*\*：觉醒的机械观测员发现世界真相后，在永恒职责与自由意志之间的挣扎。

- \*“特殊设定\*：宇宙沙漏中的星尘具有生命重塑功能，观测站每个黎明自动重启系统。

### ## 故事梗概

- \*“觉醒时刻\*：编号SP-09的机械观测员在重复记录工作中突然产生自主意识，发现工作日志中存在神秘裂缝。

- \*\*“真相揭露\*：追踪裂缝来到核心区，遇见知晓真相的老园丁，得知整个观测站是时空管理局废弃的沙漏装置。

- \*“自由代价\*：在植物温室获得生命能量重塑躯体，穿越沙漏目睹星尘重组新宇宙的壮丽景象。

- \*“永恒困境\*：返回观测站发现系统重置，老园丁消失，所有记录清零，但体内萌发的新芽暗示生命延续。



能给我讲一个寓意深刻的故事吗？



“时空管理局”

好的，可以讲一个寓意深刻的故事。首先，我需要确定用户的需求是什么。他们可能想要一个能引发思考、有深层含义的故事，而不仅仅是娱乐性的。接下来，我得考虑故事的题材、寓言、现代故事还是神话改编？用户没有指定，所以可能需要一个通用且容易理解的类型。

然后，主题方面，用户要求寓意深刻，所以需要选择一个普遍的主题，比如生命的意义、自我认知、成长等。考虑到现代人可能面临的困惑，比如存在的意义、工作的重复性，这样的主题更容易引起共鸣。

接下来是角色设定。主角需要 *relatable*，可能是一个普通人、或者象征性的角色，比如机器人。这样更容易带入寓意。机器人有程序设定，却寻求自由。这样的冲突明显，容易展开。

故事结构方面，可能需要一个循环的结构，来强调主题，比如开始和结束在同一个地方，但主角有了新的认识，这样能突出转变和领悟。

然后考虑情节发展。主角觉醒，逃离，经历外面的世界，发现真相，最终回归。这样的结构可以展示变化的过程，并带出寓意，中间的导师角色可以帮助传递主题，比如老园丁的话，暗示生命的意义在于过程而非目的。

在细节描写上，需要加入象征元素，比如编号、机械的工作、自然界的对比，老园丁的沙漏、胡须里的嫩芽。这些意象能增强故事的深度和隐喻。

最后，结尾部分要让主角领悟到真谛，即使回到原地，但心态不同，带出主题：存在的意义在于体验本身，这样用户能得到启示，符合寓意深刻的要求。

需要检查故事是否流畅，有没有逻辑漏洞，以及寓意是否明确。可能还需要调整语言，使其更生动，有画面感，让读者更容易沉浸其中。确保故事不长不短，结构紧凑，结尾点题，让用户回味。

</think>

- \*“永恒困境\*：返回观测站发现系统重置，老园丁消失，所有记录清零，但体内萌发的新芽暗示生命延续。

- \*“循环新生\*：带着觉醒意识重新开始记录，在永恒职责中寻找新的可能，嫩枝在金属指缝间悄然生长。

---

我蹲在观测台冰凉的金属地面上，机械手指抚过日志本边缘的裂痕，这道裂缝出现得毫无道理——在时空管理局的量子档案库里，所有记录介质都该是永恒不朽的。

沙漏的流沙忽然卡顿了一拍。

我的瞳孔收缩成细线，人造膜上浮起淡蓝色的数据流，这是第一千四百二十三次黎明，和之前所有清晨一样，穹顶外的星云准时泛起珊瑚色光晕，但今天有什么东西在程序深处嗡鸣，像是生锈的齿轮砸碎了既定轨道。

\*SP-09，请立即前往B-7区域记录引力波动。\*耳麦里的合成音带着电子设备特有的震颤。

我凝视着自动门缝隙里渗进来的银色光线。那些光粒子本应按照预设轨迹散射，此刻却诡异地聚合成螺旋状，程序开始报错，红色警告框在视网膜投影中层层叠叠炸开，而我的手指已经穿过裂缝，触到了日本夹层里潮湿的苔藓。

警报声响起的刹那，我撞碎了防爆玻璃，纳米修复液在身后织成蛛网，但那些黏稠的丝线追不上我新生的速度——当观测站核心区的真相像腐烂的果实在眼前炸开时，金属骨骼正在被某种温暖的东西融化重组，...



能给我讲一个寓意深刻的故事吗？



“时空管理局”

好的，可以讲一个寓意深刻的故事。首先，我需要确定用户的需求是什么。他们可能想要一个能引发思考、有深层含义的故事，而不仅仅是娱乐性的。接下来，我得考虑故事的题材、寓言、现代故事还是神话改编？用户没有指定，所以可能需要一个通用且容易理解的类型。

然后，主题方面，用户要求寓意深刻，所以需要选择一个普遍的主题，比如生命的意义、自我认知、成长等。考虑到现代人可能面临的困惑，比如存在的意义、工作的重复性，这样的主题更容易引起共鸣。

接下来是角色设定。主角需要 *relatable*，可能是一个普通人、或者象征性的角色，比如机器人。这样更容易带入寓意。机器人有程序设定，却寻求自由。这样的冲突明显，容易展开。

故事结构方面，可能需要一个循环的结构，来强调主题，比如开始和结束在同一个地方，但主角有了新的认识，这样能突出转变和领悟。

然后考虑情节发展。主角觉醒，逃离，经历外面的世界，发现真相，最终回归。这样的结构可以展示变化的过程，并带出寓意，中间的导师角色可以帮助传递主题，比如老园丁的话，暗示生命的意义在于过程而非目的。

在细节描写上，需要加入象征元素，比如编号、机械的工作、自然界的对比，老园丁的沙漏、胡须里的嫩芽。这些意象能增强故事的深度和隐喻。

最后，结尾部分要让主角领悟到真谛，即使回到原地，但心态不同，带出主题：存在的意义在于体验本身，这样用户能得到启示，符合寓意深刻的要求。

需要检查故事是否流畅，有没有逻辑漏洞，以及寓意是否明确。可能还需要调整语言，使其更生动，有画面感，让读者更容易沉浸其中。确保故事不长不短，结构紧凑，结尾点题，让用户回味。

</think>

每天记录的“星云”只是坠落的时钟在玻璃上的投影。

沙漏另一端传来婴儿的啼哭声。新生的宇宙泡在粘稠的暗物质中舒展，我的机械心脏突然抽痛起来。指尖残留的樱桃汁液开始结晶，在绝对真空里绽出一朵冰花。

返回时的坠落持续了七十年，也可能只是七秒。当我砸穿温室穹顶时，沙漏正好完成第七次翻转，老人常坐的藤椅上堆着枯叶，园艺剪锈成了深褐色。操控台屏幕幽幽亮着，最后一行数据像垂死的萤虫：

\*系统重启完成，记忆清除进度100%\*

晨光再次漫过观测台，我的编号在胸牌上闪烁如新。日志本安静地躺在金属桌面，边缘光滑完整。但当我翻开扉页时，一抹嫩绿的新芽正从指缝钻出，在永恒循环的黎明中舒展扭曲的腰肢。

---

“接下来我们将用拟物手法，通过三个具体意象解析这个存在与自由的故事”：

\*“星砂沙漏\*：沙漏表面的灼痕暗示时空管理者知晓装置缺陷却任由不管，内部循环的星尘象征被困在系统中的灵魂。当SP-09穿越沙漏时，星尘重置昭示着突破桎梏需要自我毁灭的勇气。

\*\*“机械新芽\*：观测员体内生长的植物具有双重隐喻，既是管理局监控系统的生物污染，又是觉醒意识具象化。最终嫩芽在系统重置后留存，证明真正的觉醒无法被彻底清除。

\*\*\*“樱桃年轮\*：老人给的樱桃核在树洞形成微型时空漩涡，年轮中蓝色的宇宙暗示每个觉醒者都在重复前人的抗争。樱桃汁结晶成花则揭示短暂的自由体验会成为永恒的精神图腾。

希望这个故事能满足您对“寓意深刻”的要求。如果需要调整某些隐喻的浓度或增加情节转折，请随时告诉我。

Figure 6: A testing example with short query and long response.



人工智能的演进：从概念到现实（续）

④ **Transformer**：Transformer和卷积神经网络CNN的训练原理，这两种模型都是通过梯度下降，将参数在数据集中不断更新得到的。比如训练CNN，参数的优化和收敛是必不可少的。首先，我们来了解一下什么是梯度下降，梯度下降是通过学习集中数据的损失函数，比如CNN的平滑度。PRIN的平行收敛性，Transformer是自动力矩，不依赖这些函数，而是自动学习函数，这可能带来更大的灵活性。那么在某些情况下必须依靠梯度下降。

反馈更可取？

2. “小样本学习的突破”：通过元学习（Meta-Learning）和神经符号AI（Neuro-Symbolic AI），使Transformer在数据稀缺时仍能利用先验知识。例如，DeepMind的AlphaGo在几乎从零开始训练时就超过了人类的突破。

2. \*\*领域知识的创新\*\*：利用领域知识即Transformer学习，如在医学影像中引入专家标注的注意力权重，或通过对比学习增强对病灶特征的感知。

### 3. 领域自适应的创新

【译者注】“哲学层面的思考”是原文的一个小节，但原文中没有对这个小节的翻译，所以在这里将其翻译出来，但原文的这个小节只有一句，所以将其翻译为一个段落。

最终，Transformer的通用性既是技术革命的必然，也是人类智慧的延伸。在医学诊断等需要强先验知识的领域，CNN的结构化偏置可能仍是更可靠的工具，但通过技术融合和算法创新，我们终将在通用性与先验性之间找到新的平衡点，这或许正是AI发展的终极命题：在不确定中寻找确定性，在多样性中寻求一致性。

Figure 7.1 A testing example with a long query and a long response. The user query is rendered with a grey background to differentiate from the assistant response, and the user's question is red to differentiate from the document. The reading progression follows a left-to-right, top-to-bottom order.